Aggregation of Coil–Crystalline Block Copolymers: Equilibrium Crystallization

T. Vilgis and A. Halperin*

Max Plank Institüt für Polymerforschung, Postfach 3148, D-6500 Mainz, FRG

Received June 6, 1990; Revised Manuscript Received October 9, 1990

ABSTRACT: A scaling analysis of aggregates formed by coil–crystalline diblock copolymers in a selective solvent of low molecular weight is presented. Micelles lamellae and cylinders are considered. The aggregates' cores are assumed to consist of fold crystallized blocks. The two surface tensions associated with fold crystals cause significant core anisotropy. As in rod–coil micelles, crew-cut micelles are unstable. Otherwise, the scaling behavior is similar to that of aggregates of flexible block copolymers. The cores of such aggregates, when used as seeds to induce homopolymer crystallization, may allow control of the homopolymer crystal fold size.

I. Introduction

Studies of polymer crystallization are mostly concerned with linear homopolymers.[1,2] Less attention is given to crystallization of block copolymers composed of flexible and crystallizable blocks. Yet, the crystallization of such coil–crystalline block copolymers is of interest: Aggregation of copolymers of this type gives rise to useful polymeric materials. For example, formation of crystalline micelles in a melt of crystalline–coil–crystalline triblock copolymers results in effective cross-linking, thus yielding thermotropic elastomers.[3] Also, the crystallization of homopolymers and that of block copolymers are significantly different. In particular, the crystallization of homopolymers is *kinetically* controlled, while the crystallization of block copolymers is *thermodynamically* controlled.[4] Finally, the crystallization of coil–crystalline copolymers is normally associated with aggregation into micelles, lamellae, etc. Accordingly it may be viewed as a particular form of self-assembly of amphiphilic block copolymers. As such, it is of interest because of the current activity in this field.[5–9] Experimental studies of coil–crystalline copolymers dealt mostly with gel-forming triblock copolymers in the presence or absence of solvents.[10–13] Theoretical studies focused on the lamellar phase of melts of coil–crystalline diblock copolymers.[4] In the following we analyze the *aggregation behavior of AB coil–crystalline diblock copolymers* in a *selective solvent*. The copolymers are assumed to be *monodispersed* consisting of N_A A monomers and N_B B monomers. The solvent, of *low molecular weight*, is a good solvent for the flexible A coils but a precipitant for the crystallizable B blocks. Specifically, we consider the equilibrium structure of lamellae as well as of micelles and cylinders. Such aggregates are of special interest because their cores, when used as seeds to induce crystallization of homopolymers, may allow for control of the fold size.

The overall structure of the aggregates is similar to that of all assemblies of amphiphilic block copolymers: an inner core of immiscible blocks and an outer corona of soluble, flexible blocks, swollen by the solvent. The precise geometry of the two regions depends on the particular type of aggregate considered. In any case, since we consider assemblies of incompatible blocks in a highly selective solvent, the core–corona interface is sharp. As a result, the junctions of the two blocks are constrained to the surface. Consequently, both core and coronal blocks are, in effect, grafted to the core interface, i.e., attached to the interface by a head-group only. This is an important point since densely grafted coils are strongly stretched along the normal to the surface.[14,15] The strong deformation of the flexible coronal blocks gives rise to a free energy penalty. This tends to arrest the aggregates' growth. The core's surface free energy has the opposite effect. Since the surface area per copolymer decreases as the number of aggregated copolymers grows, the surface free energy favors larger aggregates. The interplay of these two terms determines the aggregates' equilibrium structure. Our discussion so far, apart from certain omissions, applies to all types of copolymeric aggregates, irrespective of the nature of the core blocks. The distinctive features of our particular system are traceable to the core's structure. In particular, the immiscible core blocks are assumed to undergo chain-fold crystallization (Figure 1). This sets our system apart from aggregates of flexible, coil–coil, copolymers where the core is modeled as a zone of immiscible blocks in a meltlike state.[5,7,8] In a sense, the crystalline core is intermediate between the meltlike core formed by flexible immiscible blocks and the core of rod–coil aggregates where chain folding is prohibited.[16,17] In a meltlike core the blocks may adopt a multitude of ideal coil configurations. Since the core coils are flexible, they may deform upon aggregation. In turn this gives rise to a free energy penalty. In aggregates of rod–coil copolymers the configuration of the insoluble blocks is uniquely defined, independently of the aggregation state. In crystalline cores the configuration of the crystallizable blocks is adjustable. Yet the chain packing is ordered and there is no free energy change associated with the configurational adjustments. The core crystallinity also affects the equilibrium state via the following two routes: (i) The chain fold crystallization determines the packing mode of the core blocks, and this sets the relationship between the grafting density and the core's geometry. (ii) The chain fold crystallization gives rise to two different surface tensions. One is associated with the fold's plane, while the other characterizes the lateral surface which incorporates "unkinked" chain segments. In the following we obtain the aggregates equilibrium structure within the Schulman approximation, i.e., by minimizing the free energy per copolymer in a single noninteracting aggregate. The free energy per chain, F, is the sum of two terms: (i) F_{corona}, the free energy penalty due to the deformation of the densely grafted coronal blocks; and (ii) $F_{surface}$, the surface free energy associated with the core–solvent interface. The "volume" contribution to F gives rise to a constant term which plays no role in determining the equilibrium condition.

0024-9297/91/2224-2090$02.50/0

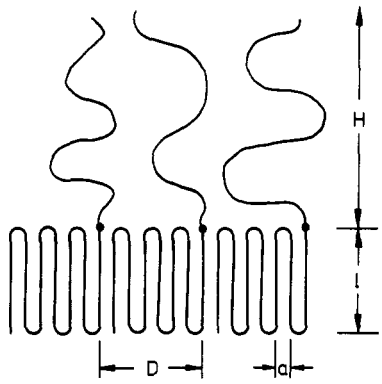

Figure 1. Schematic cross section of coil–crystalline lamella exhibiting a fold crystalline core of thickness l and a soluble corona of thickness H. In the case depicted the core consists of a single-fold crystal layer. For simplicity only the upper coronal blocks are shown.

The details of the core model are discussed in section II. It includes a description of chain packing in the core, a discussion of $F_{surface}$, and a description of the state of a single nonaggregated coil. The corona is considered in section III, where the scaling behavior of F_{corona} and the coronal dimensions are presented. The results are specified as a function of grafting density, geometry, and polymerization degree. The equilibrium characteristics of various aggregates are presented in section IV. In particular, we consider lamellae, micelles, and cylinders. Our main results are scaling laws for aggregation numbers, characteristic dimensions, etc. A brief reminder of homopolymer fold crystallization is incorporated into the discussion presented in section V. This brings out the distinctions between solution crystallization of homopolymers and block copolymers. Also, it motivates our experimental suggestions.

II. The Core

The aggregation considered takes place in highly selective solvents in which the crystallizable B blocks are insoluble. Under these conditions the B blocks are below their crystallization temperature. Accordingly, they are expected to undergo chain folding crystallization.[1,2] The resulting crystals are layered, formed by multiple folding of the chains so that the resulting segments, of length l, are aligned along the normal to the layer. The layer is bounded by two basal surfaces, "fold surfaces", where chains turn back on themselves. We assume the chains fold back at adjacent sites ("adjacent reentry") and that the number of monomers participating in the fold is small ("tight folding"). Both assumptions are reasonable for crystallization in highly selective solvents. It is important to note that the core surface incorporates two distinguishable interfaces: the fold surface and the lateral one. Each is associated with a different surface tension. In lamellar aggregates only the fold surface is of importance. However, in micellar and cylindrical aggregates both fold and lateral surfaces play an important role.

The junctions of the A and B blocks are constrained to the fold surface. In effect, the flexible A coils are grafted to the fold surface. As a result the crystals formed may consist of only one or two layers. If the A coils are grafted to both of the two fold surfaces, single-layer crystals are expected. Two-layer crystals may occur provided the A coils are somehow grafted only to one of the fold surfaces. The two scenarios are indistinguishable with respect to the scaling behavior. It is, however, important to note that in both cases layer hopping is repressed.

The assumptions of adjacent reentry and tight folding suggest that the size of the fold region, b, is comparable to monomer size, a, i.e., $b \approx a$. Since l is typically significantly larger than a, the layer thickness is essentially equal to l. We also have

$$N_B a = n_f(l + b) \approx n_f l \qquad \text{(II-1)}$$

where n_f is the number of folds (segments) per chain. The repression of layer hopping and the adjacent reentry assumption set the dimensions of the chain in the fold surface, D, to

$$D^2 \approx n_f b^2 \approx n_f a^2 \qquad \text{(II-2)}$$

Since there is one grafted A coil attached to every B block, the average separation of the grafting sites is D. Finally, the free energy per chain in an infinite chain fold crystal (ignoring edge effects) may be written[1,2,4]

$$F = n_f(E_f + lH_f) \qquad \text{(II-3)}$$

where E_f is the free energy per fold and H_f the crystal free energy per unit length. However, since $n_f l \approx N_B a$, the second term equals $N_B a H_f$, a constant playing no role in the equilibrium condition. The first term is actually identical with the contribution of the fold surface to the surface free energy per chain, $F_{surface}$. This can be seen by writing $E_f \approx b^2\sigma_f$, where σ_f is the surface tension associated with the fold surface. In the general case $F_{surface}$ incorporates two terms, allowing for the contribution of both fold and lateral surfaces.[1,2] These are endowed with surface tensions, σ_f and σ_l, with a ratio as high as $\sigma_f/\sigma_l \approx 10$.[1] The surface free energy per aggregated chain is thus of the form

$$F_{surface}/KT \approx n_f\frac{\sigma_f a^2}{kT} + \frac{S_{lateral}\sigma_l}{fkT} \qquad \text{(II-4)}$$

where $S_{lateral}$ is the lateral surface area of the core and f is the aggregation number, i.e., the number of aggregated block copolymers. The second term, while negligible in lamellae, may have important effects in micelles. These contributions also occur in the case of a single nonaggregated diblock copolymer ($f = 1$). Here the soluble A block is undeformed, retaining, essentially, the configuration of free A coil of the same size. The insoluble B block, if sufficiently long, crystallizes and forms a corelike structure. Its characteristic dimensions are set by minimizing $F_{surface}$ as given by (III-4) with $S_{lateral} \approx n_f^{1/2}al$ since $n_f a^2 \approx D^2$ and $S_{lateral} \approx Dl$. Because (II-1) leads to $l \approx N_B a/n_f$, we have $S_{lateral} \approx N_B n_f^{-1/2}a^2$ and $F_{surface}$ is given by

$$F_{surface}/kT \approx n_f\frac{\sigma_f a^2}{kT} + n_f^{-1/2}N_B\frac{\sigma_l a^2}{kT} \qquad \text{(II-5)}$$

The equilibrium condition $\partial F_{surface}/\partial n_f = 0$ yields

$$n_f \approx (N_B\sigma_l/\sigma_f)^{2/3} \qquad \text{(II-6)}$$

thus setting the "core" dimensions

$$D \approx N_B^{1/3}(\sigma_l/\sigma_f)^{1/3}a \qquad \text{(II-7)}$$

$$l \approx N_B^{1/3}(\sigma_f/\sigma_l)^{2/3}a \qquad \text{(II-8)}$$

and equilibrium free energy

$$F/kT \approx N_B^{2/3}\frac{\sigma_l^{2/3}\sigma_f^{1/3}a^2}{kT} \qquad \text{(II-9)}$$

Since the core block is essentially collapsed, its dimensions scale as $N_B^{1/3}$, as expected. Yet, significant unisotropy

may occur because $D/l \approx \sigma_t/\sigma_f$ and σ_f/σ_l may be rather large.

III. The Corona

The aggregates' exterior corona consists of soluble A coils swollen by the solvent. Since the A–B junctions are constrained to the core–solvent interface, the A blocks are, in effect, grafted to the core's surface. The structure and characteristic properties of a grafted layer are determined by its geometry, the grafting density and the polymerization degree of the grafted coils, N_A. The details of the core model are indirectly discernible through the grafting density and the geometry of the core. However, for a given set of characteristic attributes the coronal structure is independent of the core model. The coronal structure is obtainable by means of a blob ansatz.[14,18,19] The corona is pictured as a semidilute solution comprising close packed blobs. The blobs are arranged in layers, shaped in accordance with the coronal geometry. Thus, a flat corona comprises plane layers, while a spherical corona consists of concentric spherical shells. Within a given layer the blobs are of equal size. A grafted chain contributes one blob to each layer. This last requirement accounts for the stretched configurations adopted by densely grafted chains. For a flat corona the area of each layer, S, is a constant. The blob size, ξ, is thus given by $f\xi^2 \approx S$ or $\xi \approx D$, where D is the average separation between grafting sites. In the case of a cylindrical corona of length L the area of a layer is position dependent. In particular, $S \approx rL$ and thus $f\xi^2 \approx rL$ or $\xi \sim (rL/f)^{1/2}$. For spherical coronas we have $S \approx r^2$, leading to $f\xi^2 \approx r^2$ or $\xi \sim r/f^{1/2}$. Knowledge of ξ allows us to obtain the coronal thickness, H, and the free energy per grafted coronal block, F_{corona}. Mass conservation determines the coronal thickness. A blob of size ξ contains $g \approx (\xi/a)^{5/3}$ monomers. In a flat corona where $\xi \approx D$, we immediately have $H \approx (N_A/g)D \approx N_A(a/D)^{2/3}a$. For the cylindrical and spherical cases we have

$$N_A \approx \int_{R_{in}}^{R_{in}+H} (\xi/a)^{5/3}\xi^{-1}\,dr \qquad \text{(III-1)}$$

where R_{in} is the radius of the grafted surface. In the limit considered, of $H \gg R_{in}$, eq III-1 yields $H \approx (fa/L)^{1/4}N_A^{3/4}a$ for the cylindrical case and $H \approx f^{1/5}N_A^{3/5}a$ for the spherical one. The kT per blob prescription yields the free energy per grafted coronal chain, F_{corona}. For a flat corona the number of blobs per chain is H/D, and thus $F_{corona}/kT \approx H/D \approx N_A(a/D)^{5/3}$. In the other geometries, with blobs of variable size, F_{corona} is given by

$$F_{corona}/kT \approx \int_{R_{in}}^{R_{in}+H} \xi^{-1}\,dr \qquad \text{(III-2)}$$

The one-dimensional form of (III-1) and (III-2) reflects the stretched configurations of the densely grated chains. Equation III-2 leads to $F_{corona}/kT \approx f^{1/2}\ln(R_{in}+H)/R_{in}$ for spherical coronas. In this case we typically approximate the logarithmic factor as a constant leading to $F_{corona}/kT \approx f^{1/2}$. In the limit of $H \gg R_{in}$ (II-2) leads to $F_{corona}/kT \approx (fH/L)^{1/2}$ for cylindrical coronas. In such cases we also have $H \approx (fa/L)^{1/4}N_A^{3/4}a$, thus leading to $F_{corona} \approx (fa/L)^{5/8}N_A^{3/8}$. These and all other relevant results are summarized in Table I.

IV. Equilibrium Characteristics of Lamellae and Micelles

In the following we consider three types of aggregates: lamellae, micelles, and cylinders. In the micellar cases we also distinguish between crew-cut micelles, with a corona

Table I
Scaling Behavior of Flat Cylindrical and Spherical Grafted Layers in a Good Solvent

geometry	ξ	H/a	F_{corona}/kT
flat	D	$N_A(a/D)^{2/3}$	$N_A(a/D)^{5/3}$
cylindrical	$(rL/f)^{1/2}$	$(fa/L)^{1/4}N_A^{3/4}$	$(fa/L)^{5/8}N_A^{3/8}$
spherical	$r/f^{1/2}$	$f^{1/5}N_A^{3/5}$	$f^{1/2}\ln(R_{in}+H)/R_{in} \approx f^{1/2}$

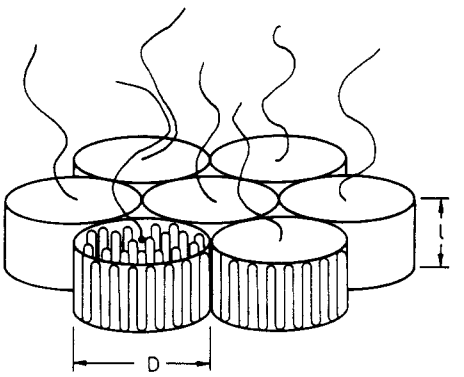

Figure 2. Schematic representation of coil–crystalline lamella. For simplicity the crystalline blocks are depicted as cylinders with a coronal block attached to the bases' centers. In reality other geometries are allowed provided they exhibit the same scaling properties.

reminiscent of flat grafted layers, and starlike micelles, where the corona adopts the structure of spherical grafted layers. Within the Schulman approximation the equilibrium state is determined by minimizing F, the free energy per chain.

$$F = F_{surface} + F_{corona} \qquad \text{(IV-1)}$$

The general form of $F_{surface}$ is given by (III-4). The form adopted for $S_{lateral}$ in the second term of $F_{surface}$ reflects the special features of each type of aggregate. F_{corona} is chosen from Table I according to geometry of the coronal layer. The lamellar aggregates are simplest to analyze (Figure 2). In this case the corona is similar to a flat grafted layer. The combination of $F_{corona}/kT \approx N_A(a/D)^{5/3}$ (Table I) and $D \approx n_f^{1/2}a$ (II-2) leads to $F_{corona}/kT \approx N_A n_f^{-5/6}$. The second term in eq II-4 is negligible in the lamellar case and $F_{surface}/kT \approx n_f(\sigma_f a^2/kT)$. Altogether we have

$$F/kT \approx n_f\frac{\sigma_f a^2}{kT} + N_A n_f^{-5/6} \qquad \text{(IV-2)}$$

Minimization with respect to n_f yields

$$n_f \approx N_A^{6/11}(kT/\sigma_f a^2)^{6/11} \qquad \text{(IV-3)}$$

Use of (II-1), (II-2), and Table I leads to the following expressions for the equilibrium values at l, D, and H:

$$l/a \approx N_B N_A^{-6/11}(\sigma_f a^2/kT)^{6/11} \qquad \text{(IV-4)}$$

$$D/a \approx N_A^{3/11}(kT/\sigma_f a^2)^{3/11} \qquad \text{(IV-5)}$$

$$H/a \approx N_A^{9/11}(\sigma_f a^2/kT)^{2/11} \qquad \text{(IV-6)}$$

and to the equilibrium value of the lamellar F

$$F/kT \approx N_A^{6/11}(\sigma_f a^2/kT)^{5/11} \qquad \text{(IV-7)}$$

The scaling behavior of D, H, and F is essentially that of saturated monolayer of diblock copolymers at a liquid interface.[14] In both cases the equilibrium condition reflects the interplay between $F_{surface}$ and F_{corona} with no core contribution. In this case only σ_f plays a role. As a result

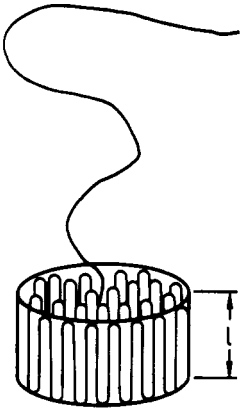

Figure 3. Schematic picture of a single coil–crystalline diblock copolymer in a selective solvent. The insoluble crystallizable block underwent fold crystallization.

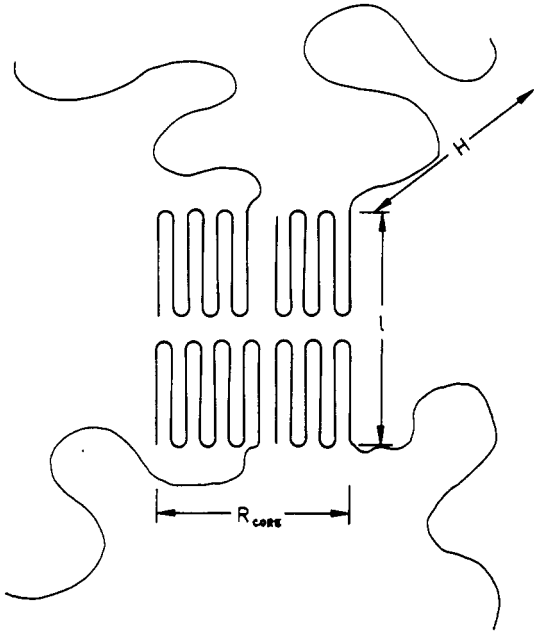

Figure 4. Schematic cross section of starlike coil–crystalline micelle exhibiting a double stack of fold crystallized core blocks and carrying extended coronal blocks.

one expects no special features due to the crystallizable blocks.

We next consider the equilibrium characteristics of spherical micelles. This term is somewhat misleading. It is chosen because of the similarity between these micelles and the spherical micelles formed by the flexible coil–coil block copolymers. However, in our case the cores are actually cylindrical. The bases, comprising the fold surfaces, carry each a coronal "mop" (Figure 4). When the coronal blocks are long enough, the corona is reminiscent of spherical grafted layer and the micelle as a whole is nearly spherical. Because of the similarity between such coronal mops and star polymers, we refer to these moieties as "starlike micelles". One may also imagine "crew-cut micelles" in which the coronal blocks are short and the coronal mops are similar to flat grafted layers. Such micelles are not spherical, but the introduction of a better term is unnecessary since, as we shall see, such micelles are unstable. Irrespective of the coronal structure the core radius, R_{core}, is given by $R_{core} \approx f^{1/2}D \approx f^{1/2}n_f^{1/2}a$, leading to $S_{lateral} \approx f^{1/2}n_f^{1/2}al$ or, by (II-1), $f^{-1}S_{lateral} \approx N_B f^{-1/2}n_f^{-1/2}a^2$. Accordingly, $F_{surface}$ is given by

$$F_{surface}/kT \approx n_f\frac{\sigma_f a^2}{kT} + N_B f^{-1/2}n_f^{-1/2}\frac{\sigma_f a^2}{kT} \quad \text{(IV-8)}$$

For crew-cut micelles $F_{corona}/kT \approx N_A(a/D)^{5/3} \approx N_A n_f^{-5/6}$ and

$$F/kT \approx N_A n_f^{-5/6} + n_f\frac{\sigma_f a^2}{kT} + N_B f^{-1/2}n_f^{-1/2}\frac{\sigma_f a^2}{kT} \quad \text{(IV-9)}$$

In this case the equilibrium condition is $\partial F/\partial n_f = \partial F/\partial f = 0$. Since only one of the terms in (IV-9) is f dependent, $\partial F/\partial f = 0$ leads to

$$f = \infty \quad \text{(IV-10)}$$

indicating a tendency to form lamellae. A similar tendency is found in crew-cut micelles of rod–coil diblock copolymers.[17] In both cases it reflects the absence of penalty term associated with the deformation of the core blocks upon aggregation.

For starlike micelles $F_{corona}/kT \approx f^{1/2}$ and F is given by

$$F/kT \approx f^{1/2} + n_f\frac{\sigma_f a^2}{kT} + N_B f^{-1/2}n_f^{-1/2}\frac{\sigma_f a^2}{kT} \quad \text{(IV-11)}$$

As opposed to the case of crew-cut micelles, the equilibrium condition, $\partial F/\partial n_f = \partial F/\partial f = 0$, now yields a stable, finite micelle. In particular

$$\frac{\sigma_f a^2}{kT} + N_B^{-1/2}n_f^{-3/2}\frac{\sigma_f a^2}{kT} = 0 \quad \text{(IV-12)}$$

$$f^{-1/2} - N_B f^{-3/2}n_f^{-1/2}\frac{\sigma_f a^2}{kT} = 0 \quad \text{(IV-13)}$$

lead to the equilibrium f and n_f

$$f \approx N_B^{4/5}\left(\frac{\sigma_f a^2}{kT}\right)^{4/5}\left(\frac{\sigma_f a^2}{kT}\right)^{2/5} \quad \text{(IV-14)}$$

$$n_f \approx N_B^{2/5}\left(\frac{\sigma_f a^2}{kT}\right)^{2/5}\left(\frac{kT}{\sigma_f a^2}\right)^{4/5} \quad \text{(IV-15)}$$

For starlike micelles the coronal thickness, H, sets the overall micellar radius, R. By using $H \approx f^{1/5}N_A^{3/5}a$ (Table I) we obtain

$$R \sim H \sim N_B^{4/25}N_A^{3/5} \quad \text{(IV-16)}$$

Equations II-1 and II-2 lead to

$$l/a \approx N_B^{3/5}\left(\frac{kT}{\sigma_f a^2}\right)^{2/5}\left(\frac{\sigma_f a^2}{kT}\right)^{4/5} \quad \text{(IV-17)}$$

$$D/a \approx N_B^{1/5}\left(\frac{\sigma_f a^2}{kT}\right)^{1/5}\left(\frac{kT}{\sigma_f a^2}\right)^{2/5} \quad \text{(IV-18)}$$

and, since $R_{core} \approx f^{1/2}D$, to

$$R_{core} \approx N_B^{3/5}\left(\frac{\sigma_f a^2}{kT}\right)^{3/5}\left(\frac{kT}{\sigma_f a^2}\right)^{1/5} \quad \text{(IV-19)}$$

Finally, the equilibrium F is given by

$$F/kT \approx N_B^{2/5}\left(\frac{\sigma_f a^2}{kT}\right)^{2/5}\left(\frac{\sigma_f a^2}{kT}\right)^{1/5} \quad \text{(IV-20)}$$

The scaling behavior found for starlike micelles is identical

with that of micelles formed by flexible diblock copolymers.[7] In both cases the equilibrium state is due to the balance of $F_{surface}$ and F_{corona} with core blocks of adjustable configurations. Different results are obtained for starlike micelles formed by rod–coil copolymers because the configuration of the core blocks, in this system, is unchangeable.[17] Yet starlike micelles of coil–crystalline copolymers possess two distinct properties: (i) The micellar core can be highly unisotropic since $R/l \approx \sigma_l/\sigma_f$ and σ_f/σ_l can be of order 10.[1] In micelles formed by flexible copolymers the core is expected to be spherical. (ii) The crystalline core blocks all adopt anisotropic configurations characterized by $D/l \approx N_B^{-2/5}(\sigma_l/\sigma_f)^{3/5}(kT/\sigma_f a^2)^{3/5}$. In marked contrast, most of the core blocks in micelles of flexible copolymers assume ideal coil configurations. Only a minority of the chains are deformed.[20]

One may view cylindrical aggregates as intermediate between lamellae and micelles. Again, the term is chosen because of the analogy to cylindrical aggregates formed by flexible block copolymers. However, in our case the core is a square prizm, assumed to be of infinite length. The two prizms' bases, of width w, incorporate the fold surfaces. Each carries grafted A chains such that the average separation between grafting sites is D (for a cylinder of finite length L we have $D = L/f$). The folds' length, l, sets the core height. We assume the chains aggregate into a linear array. Each immiscible B block occupies a volume Dwl such that

$$\mathrm{Dwl} \approx N_B a^3 \tag{IV-21}$$

Also, any given B block has two adjacent neighboring B blocks of identical volume. The fold surface area per chain is now given by Dw, and eq II-2 is thus replaced by

$$n_f a^2 \approx \mathrm{Dw} \tag{IV-22}$$

These relations are supplemented by eq II-1, $n_f l \approx N_B a$, which remains unmodified. The lateral surface area per chain, $f^{-1}S_{lateral}$ is

$$f^{-1}S_{lateral} \approx \mathrm{Dl} \approx n_f^{-1}(D/a)N_B a^2 \tag{IV-23}$$

and the free energy per aggregated chain, obtained by combining eq IV-1, II-4, and IV-23 is thus given by

$$F/kT \approx n_f\left(\frac{\sigma_f a^2}{kT}\right) + n_f^{-1}(D/a)N_B\left(\frac{\sigma_l a^2}{kT}\right) + (a/D)^{5/8}N_A^{3/8} \tag{IV-24}$$

The last term, F_{corona}, is obtained from Table I by using $L/f \approx D$. The cylinder's equilibrium characteristics are set by the conditions $\partial F/\partial D = \partial F/\partial n_f = 0$ or

$$-n_f^{-1}N_B\frac{\sigma_l a^2}{kT} + (a/D)^{13/8}N_A^{3/8} = 0 \tag{IV-25}$$

$$\frac{\sigma_f a^2}{kT} - n_f^{-2}(D/a)N_B\frac{\sigma_l a^2}{kT} = 0 \tag{IV-26}$$

leading to

$$D/a \approx N_A^{1/3}N_B^{-4/9}[kT/(\sigma_l\sigma_f)^{1/2}a^2]^{8/9} \tag{IV-27}$$

and

$$n_f \approx N_A^{1/6}N_B^{5/18}[kT/(\sigma_l\sigma_f)^{1/2}a^2]^{4/9}(\sigma_l\sigma_f)^{1/2} \tag{IV-28}$$

(II-1) and (IV-28) yield the equilibrium l

$$l/a \approx N_A^{-1/6}N_B^{13/18}[(\sigma_l\sigma_f)^{1/2}a^2/kT]^{4/9}(\sigma_f\sigma_l)^{1/2} \tag{IV-29}$$

Knowing n_f and D we obtain w via eq IV-22

$$w/a \approx N_A^{1/6}N_B^{13/18}[(\sigma_l\sigma_f)^{1/2}a^2/kT]^{4/9}(\sigma_l/\sigma_f)^{1/2} \tag{IV-30}$$

R as given in Table I may be rewritten as $R \approx (a/D)^{1/4}N_A^{3/4}a$, leading to

$$R/a \approx N_A^{2/3}N_B^{1/9}[(\sigma_l\sigma_f)^{1/2}a^2/kT]^{2/9} \tag{IV-31}$$

The equilibrium form of F is given by

$$F/kT \approx N_A^{1/6}N_B^{5/18}[(\sigma_l\sigma_f)^{1/2}a^2/kT]^{5/9} \tag{IV-32}$$

Apart from the caveats listed earlier, similar scaling behavior is expected in cylinders formed by flexible block copolymers.

V. Discussion

The crystalline cores of block copolymer aggregates are of special interest because they differ from homopolymer crystals. The lamellar thickness, l, of homopolymer crystals is thought to be kinetically controlled.[1,2] In particular, l is set by the kinetics of secondary nucleation, i.e., the onset of fold crystallization on a flat surface of an existing fold crystal, present because of seeding or primary nucleation. The secondary nucleus consists of a monomer thick layer comprising ν folds of length l and width a. Since the crystallizing chain is in contact with a surface of fold crystal, the excess free energy of formation, ΔF, is given by

$$\Delta F = 2\nu a^2\sigma_f + 2al\sigma_l - \nu a^2 l\Delta f \tag{V-1}$$

where Δ_f is the free energy per unit volume of the crystal. A rough estimate of l equates it to l of the critical nucleus, l^*, obtained by setting $\partial\Delta F/\partial l = \partial\Delta F/\partial\nu = 0$, leading to $l^* = 2\sigma_f/\Delta f$. More detailed kinetic theories lead to

$$l = \frac{2\sigma_f}{\Delta f} + \delta l \tag{V-2}$$

where δl is a function of T, σ_l, σ_f, and H_f.

The following feature is especially important: The material properties determining l are σ_f, σ_l, and Δf. The molecular weight plays no role. In marked contrast the solution crystallization of diblock copolymers is thermodynamically controlled, i.e., there exists a unique set of crystallization parameters corresponding to a minimum in the appropriate free energy. Also, the fold length l is a strong function of the block polymerization degrees, N_A and N_B. This allows one to tune l for a given set of σ_f, σ_l, Δf, and T. Furthermore, the crystalline cores of copolymeric aggregates may afford novel control options when used as seeds to induce crystallization of homopolymers. The secondary nucleation is usually assumed to take place on an infinite surface, i.e., a surface of dimensions much larger than the fold size of the secondary nucleus. The surface plays no role in determining the fold size apart from lowering the nucleation free energy barrier. In marked distinction the crystalline core provides a nucleation strip rather than a nucleation surface. The strip height is adjustable and can be made smaller than the nucleus fold size expected on an unbounded surface. Under these conditions the secondary nucleus fold size is expected to match the strip height. Larger folds will be penalized with higher nucleation barriers due to excess surface free energy. Accordingly the use of crystalline cores as seeds may allow us to control the fold size of homopolymer crystals and to enforce deviations from eq V-2. Such aggregates are also interesting as an example of self-assembly of polymeric surfactons. The fold crystalline core is an intermediate case with respect to cores formed

by flexible coils and those consisting of rigid rods. In particular, the core blocks may adjust their configuration; however, there is no free energy penalty associated with such deformations. As a result coil–crystalline aggregates exhibit the scaling behavior of aggregates formed by flexible copolymers, the exception being the lack of stability of crew-cut micelles, which is reminiscent of the behavior of rod–coil aggregates. Another interesting feature is the cores' unisotropy in micelles and cylinders. This trait reflects the interplay of two very different surface tensions characterizing the two types of core surfaces. Finally, the configurations of all core blocks are expected to be strongly anisotropic in marked distinction to the state of amorphous flexible core blocks.

The experimental work in this area was mostly directed at crystal–coil–crystal triblock copolymers. Since these tend to form gels, a direct comparison with our results is impossible. However, the gels investigated did contain aggregates of the types considered by us. Our analysis suggests the study of aggregates formed by coil–crystal diblock copolymers. Care must be taken to anneal aggregates so as to allow them to attain equilibrium state.

Acknowledgment. It is a pleasure to acknowledge useful discussions with Prof. H. Benoit and with Prof. E. W. Fischer, who acquainted us with refs 10–13, thus motivating the study. A.H. is grateful for the hospitality of Prof. E. W. Fischer and the Max Planck Institut für Polymerforschung.

References and Notes

(1) Wunderlich, B. *Macromolecular Physics*; Academic Press: New York, 1976.
(2) Basset, D. C. *Principles of Polymer Morphology*; Cambridge University Press: Cambridge, U.K., 1981.
(3) Mark, J. E.; Erman, B. *Rubberlike Elasticity—A Molecular Primer*; Wiley: New York, 1988.
(4) Whitmore, M. D.; Noolandi, J. *Macromolecules* **1988**, *21*, 1482. (b) Whitmore, M. D.; Noolandi, J. *Makromol. Chem., Makromol. Symp.* **1987**, *16*, 235.
(5) Marques, C.; Joanny, J. F.; Leibler, L. *Macromolecules* **1988**, *21*, 1051.
(6) Bug, A. L. R.; Cates, M. E.; Safran, S. E.; Witten, T. A. *J. Chem. Phys.* **1987**, *87*, 824.
(7) Halperin, A. *Macromolecules* **1987**, *20*, 2934.
(8) Birshtein, T. M.; Zhulina, E. B. *Polymer* **1989**, *30*, 170.
(9) Munch, M. R.; Gast, A. P. *Macromolecules* **1988**, *21*, 1360, 1366.
(10) Skoulios, A. E.; Tsouladze, G.; Franta, E. *J. Polym. Sci., Part C* **1963**, *4*, 507.
(11) Franta, E.; Skoulios, A. E.; Rempp, P.; Benoit, H. *Makromol. Chem.* **1965**, *87*, 271.
(12) Lotz, B.; Kovacs, A. J. *Polym. Prepr.* **1969**, *10* (2), 820.
(13) (a) Geravais, M.; Gallot, B. *Macromol. Chem.* **1973**, *171*, 157; (b) **1973**, *174*, 193; (c) **1977**, *178*, 1577; (d) **1977**, *178*, 2071; (e) **1979**, *130*, 2041.
(14) Alexander, S. *J. Phys.* (*Paris*) **1977**, *38*, 977.
(15) de Gennes, P. G. *Solid State Phys.* **1978**, *14*, 1.
(16) Halperin, A. *Europhys. Lett.* **1989**, *10*, 549.
(17) Halperin, A. *Macromolecules* **1991**, in press.
(18) (a) Daoud, M.; Cotton, J. P. *J. Phys.* (*Paris*) **1982**, *43*, 531. (b) Witten, T. A.; Pincus, P. A. *Macromolecules* **1986**, *19*, 2509.
(19) Wang, Z. G.; Safran, S. A. *J. Chem. Phys.* **1988**, *89*, 5323.
(20) Semenov, A. N. *Sov. Phys.—JETP* (*Engl. Transl.*) **1985**, *61*, 733.